

2016-07-08

Seasonal sea ice variability in eastern Fram Strait over the last 2000years

Cabedo-Sanz, P

<http://hdl.handle.net/10026.1/5102>

10.1007/s41063-016-0023-2

arktos

Springer Science and Business Media LLC

All content in PEARL is protected by copyright law. Author manuscripts are made available in accordance with publisher policies. Please cite only the published version using the details provided on the item record or document. In the absence of an open licence (e.g. Creative Commons), permissions for further reuse of content should be sought from the publisher or author.

Seasonal sea ice variability in eastern Fram Strait over the last 2,000 years

Patricia Cabedo-Sanz and Simon T Belt*

School of Geography, Earth and Environmental Sciences, Plymouth University,
Drake Circus, Plymouth, PL4 8AA, UK

* Author for correspondence

Professor Simon T Belt
Plymouth University
Drake Circus, Plymouth
PL4 8AA
UK

e-mail: sbelt@plymouth.ac.uk
Phone: +44 (0)1752 584959
FAX: +44 (0)1752 584709

Keywords: IP₂₅; sea ice; biomarker; proxy; Late Holocene; Fram Strait

1 **Abstract**

2

3 We present a high-resolution (ca. 50 yr) biomarker-based reconstruction of seasonal
4 sea ice conditions for the West Svalbard continental margin covering the last ca. 2
5 kyr. Our reconstruction is based on the distributions of sea ice algal (IP₂₅) and
6 phytoplankton (brassicasterol and HBI III) lipids in marine sediment core MSM5/5-
7 712-1 retrieved in 2007. The individual and combined (PIP₂₅) temporal profiles,
8 together with estimates of spring sea ice concentration (SpSIC (%)) based on a
9 recent calibration, suggest that sea ice conditions during the interval ca. 50-1700 AD
10 may not have been as variable as described in previous reconstructions, with SpSIC
11 generally in the range ca. 35-45%. A slight enhancement in SpSIC (ca. 50%) was
12 identified at ca. 1600 AD, contemporaneous with the Little Ice Age, before declining
13 steadily over the subsequent ca. 400 years to near-modern values (ca. 25%). In
14 contrast to these spring conditions, our data suggest that surface waters during
15 summer months were ice-free for the entire record. The decline in SpSIC in recent
16 centuries is consistent with the known retreat of the winter ice margin from
17 documentary sea ice records. This decrease in sea ice is possibly attributed to
18 enhanced inflow of warm water delivered by the North Atlantic Current and/or
19 increasing air temperatures, as shown in previous marine and terrestrial records.
20 Comparison of our biomarker-based sea ice reconstruction with one obtained
21 previously based on dinocyst distributions in a core from a similar location, reveals
22 partial agreement in the early-mid part of the records (ca. 50–1700 AD), but a
23 notable divergence in the most recent ca. 300 years. We hypothesise that this
24 divergence likely reflects the individual signatures of each proxy method, especially
25 as the biomarker-based SpSIC estimates during this interval (<25%) are much lower

26 than the threshold level (>50% sea ice cover) used for the dinocyst approach.
27 Alternatively, divergence between outcomes may indicate seasonality shifts in sea
28 ice conditions, such that a combined biomarker-dinocyst approach in future studies
29 might provide further insights into this important parameter.

30

31 **1. Introduction**

32

33 *1.1 Sea ice and the study region*

34

35 Sea ice is a critical component of the global climate system, influencing heat, gas
36 and moisture exchange between the oceans and the atmosphere (Thomas and
37 Dieckmann 2010), and further contributing to circulation patterns through brine
38 rejection and freshwater release during ice formation and melt, respectively (e.g.
39 Dickson et al. 2007 and references therein). The observed rapid decline in Arctic sea
40 ice extent and thickness (e.g. Stroeve et al. 2012) has prompted a need to better
41 resolve temporal changes to sea ice in the past, in order that the recent trends can
42 be placed into a better context, and to provide key datasets for improving models of
43 past and future change (e.g. Goosse et al. 2013; Johannessen et al. 2004). From a
44 regional perspective, Fram Strait represents a pivotal study location for investigating
45 past changes to sea ice since it represents the major oceanographic gateway
46 between the Arctic and North Atlantic oceans (Fig. 1a). The two main currents that
47 characterize the region are the North Atlantic Current (NAC) and the East Greenland
48 Current (EGC) (Fig. 1a). Northerly flowing warm Atlantic Water is delivered to the
49 Arctic by the NAC via a principal trajectory along the West Svalbard continental
50 margin, which normally renders eastern Fram Strait relatively free of sea ice, even in

51 winter. In contrast, western Fram Strait is characterized by cold, ice-laden waters as
52 a result of sea ice export from the Arctic Ocean via the EGC. Arctic Water also flows
53 along the east coast of Svalbard to the south and west of Spitsbergen, delivering sea
54 ice via the East Spitsbergen Current (ESC) (Hopkins 1991; Loeng 1991). The
55 magnitude of heat delivery by the NAC plays a critical role in determining the precise
56 sea ice conditions in eastern Fram Strait. For example, increased Atlantic Water
57 inflow during the last ca. 120 years (Spielhagen et al. 2011) has been associated
58 with a general trend of reduced sea ice cover in the Arctic and, more locally, a
59 northerly retreat of the winter ice margin (Fig. 1b, Divine and Dick 2006). A further
60 impact of the NAC on sea ice conditions in the region, more generally, is that
61 seasonal shifts in the position of the winter and summer ice margins are significantly
62 less pronounced than for the central and eastern Barents Sea, which are dominated
63 by low temperature and salinity Arctic Water (Hopkins 1991). The latter regions also
64 experience seasonal ice cover from autumn to spring, before retreating, rapidly,
65 during late spring/summer. As such, the region as a whole experiences contrasting
66 seasonal sea ice cover (Vinje 1975), which is influenced, in part, by the strength of
67 the NAC (Hopkins 1991).

68

69 Motivated, in part, by the sensitivity of oceanographic and atmospheric conditions in
70 Fram Strait towards climatic change, a number of proxy-based studies have been
71 carried out in recent years that have provided new insights into the centennial- and
72 millennial-scale paleoceanographic evolution along the West Svalbard continental
73 margin (e.g. Bonnet et al. 2010; Jernas et al. 2013; Müller and Stein 2014; Müller et
74 al. 2012; Spielhagen et al. 2011; Werner et al. 2013). These investigations have
75 benefited from the recovery of high accumulation rate (and well-dated) marine

76 sediments, which have enabled the application of an array of biological and
77 mineralogical proxies for the determination of atmospheric and oceanic
78 temperatures, salinity, and sea ice cover (Bonnet et al. 2010; Müller and Stein 2014;
79 Müller et al. 2012; Rueda et al. 2013; Spielhagen et al. 2011; Werner et al. 2011).

80

81 Our objective in the current study is to add to the existing suite of previous
82 paleoceanographic investigations for West Svalbard, by presenting a high-resolution
83 (ca. 50 yr) biomarker-based reconstruction of sea ice conditions spanning the last
84 ca. 2 kyr. In particular, we build on recent developments in biomarker-based
85 approaches to sea ice reconstruction by providing both descriptive and semi-
86 quantitative estimates of spring sea ice concentration (SpSIC (%)). Biomarker-based
87 sea ice reconstructions for the West Svalbard margin have been performed
88 previously through analysis of sediments from the same or similar locations,
89 although these focused mainly on longer timeframes (e.g. Holocene and post-LGM;
90 Müller et al. 2012, 2014) and did not provide information for recent centuries. In
91 addition, semi-quantitative estimates of SpSIC were only tentative (Müller et al.
92 2012). A dinocyst-based record of mean annual sea ice duration (months/yr) for the
93 last 2 kyr for West Svalbard has previously been presented by Bonnet et al. (2010),
94 however, and we make comparisons between this and our biomarker-based record
95 as part of the current study.

96

97 *1.2 Background to biomarker proxy method*

98

99 In recent years, the organic geochemical marker IP₂₅ (Ice Proxy with 25 carbon
100 atoms; Belt et al. 2007) has emerged as a particularly suitable proxy method for

101 carrying our Arctic sea ice reconstructions, and in the determination of past seasonal
102 sea ice cover, in particular (e.g. Belt and Müller 2013; Belt et al. 2010; Berben et al.
103 2014; Cabedo-Sanz et al. 2013; Stein et al. 2012). IP₂₅ is a mono-unsaturated highly
104 branched isoprenoid (HBI) lipid produced by certain Arctic sea ice diatoms (Brown et
105 al. 2014), and is found commonly in Arctic and sub-Arctic marine sediments
106 underlying seasonal sea ice cover (Müller et al. 2011; Navarro-Rodriguez et al. 2013;
107 Stoyanova et al. 2013; Xiao et al. 2013, 2015). Identification of IP₂₅ in the geological
108 record (Arctic marine sediments) therefore provides a convincing case for the past
109 occurrence of seasonal sea ice, while variability in IP₂₅ content is generally
110 associated with corresponding fluctuations in seasonal sea ice extent (e.g. Belt and
111 Müller 2013). The absence of IP₂₅ in Arctic and sub-Arctic settings is less
112 straightforward to interpret, although either of permanent ice cover or ice-free
113 conditions have been suggested as potential settings (e.g. Belt and Müller 2013;
114 Stein et al. 2012; Xiao et al. 2015). In any case, the co-measurement of certain
115 phytoplankton biomarkers (including sterols such as brassicasterol) can provide
116 additional information about low-ice or open-water conditions. In addition, combining
117 IP₂₅ and phytoplankton marker concentrations in the form of the so-called PIP₂₅
118 index (Müller et al. 2011) has the potential to provide even more detailed or semi-
119 quantitative estimates of sea ice conditions than from the individual biomarkers
120 alone. The use of brassicasterol as a phytoplankton biomarker when calculating
121 PIP₂₅ indices is not without problems, however, since it may also be derived from
122 non-marine sources, and its (generally) much higher sedimentary abundance
123 necessitates the use of a balance factor in the PIP₂₅ calculation (see Section 2.2),
124 which can cause problems of consistency, in particular (see Belt and Müller, 2013;
125 Belt et al. 2015 for further details). Since these limitations may not be relevant in all

126 cases, the adoption of a further phytoplankton marker, possessing a more selective
127 source and which has sedimentary concentrations closer to those of IP₂₅, might
128 represent a suitable complementary approach, at least. Indeed, Belt et al. (2015)
129 recently demonstrated that a further tri-unsaturated HBI lipid (C_{25:3} or HBI III) derived
130 from certain diatoms may be a more suitable phytoplankton marker for use within the
131 PIP₂₅ index, following analysis of lipid distributions in surface sediments from the
132 Barents Sea experiencing variable seasonal sea ice cover. Smik et al. (2016)
133 subsequently showed that PIP₂₅ indices based on IP₂₅ and HBI III (i.e. P_{III}IP₂₅) exhibit
134 a strong linear correlation to SpSIC in the Barents Sea, thus providing a potential
135 means of reconstructing semi-quantitative SpSIC (%) estimates for this region, at
136 least. In the current study, we therefore measured concentrations of IP₂₅,
137 brassicasterol and HBI III in a ¹⁴C-dated sediment core (MSM5/5-712-1) retrieved
138 from the West Svalbard margin in 2007 and used P_{III}IP₂₅ indices together with the
139 recent calibration of Smik et al. (2016) to obtain estimates of SpSIC (%) for the last 2
140 kyr.

141

142 **2. Material and methods**

143

144 *2.1 Field methods and chronology*

145

146 Core MSM5/5-712-1 was recovered from the West Svalbard continental margin
147 (78°54.94 N, 6°46.04 E, water depth 1490.5 m, core length 46 cm; Fig 1a) during
148 cruise leg MSM5/5 on board the R/V *Maria S. Merian* in the summer of 2007. The
149 age model is based on five ¹⁴C accelerator mass spectrometry (AMS) radiocarbon
150 dates presented and described previously (Spielhagen et al. 2011).

151

152 *2.2 Biomarker analyses*

153

154 In total, 43 downcore sediment samples were analysed for the biomarkers IP₂₅, HBI
155 III and brassicasterol. Sampling and analysis was carried out at 1 cm intervals
156 representing the last ca. 2 kyr, with a resolution of ca. 50 yr. Biomarker analyses
157 (HBI and sterol lipids) were performed using methods described previously (Belt et
158 al. 2012, 2015). Briefly, two internal standards were added to each freeze-dried
159 sediment sample to permit quantification of lipid biomarkers. 9-octylheptadec-8-ene
160 (9-OHD, 10 µL; 10 µg mL⁻¹) was added for quantification of HBI lipids (IP₂₅ and HBI
161 III), while 5α-androstan-3β-ol (10 µL; 10 µg mL⁻¹) was added for quantification of
162 brassicasterol. Samples were then extracted using dichloromethane/methanol (3 x 3
163 mL; 2:1 v/v) and ultrasonication. Following removal of the solvent from the combined
164 extracts using nitrogen, the resulting total organic extracts (TOE) were purified using
165 column chromatography (silica), with HBIs (hexane; 6 mL) and brassicasterol (20:80
166 methylacetate/hexane ; 6 mL) collected as two fractions. Analysis of individual
167 fractions was carried out using gas chromatography-mass spectrometry (GC-MS)
168 and operating conditions were as described previously (e.g. Belt et al. 2012; Brown
169 and Belt 2012). Brassicasterol was derivatized (BSTFA; 50 µL; 70°C; 1h) prior to
170 analysis by GC-MS. Mass spectrometric analyses were carried out either in total ion
171 current (TIC) or single ion monitoring (SIM) mode. The identification of IP₂₅ (Belt et
172 al. 2007) and HBI III (Belt et al. 2000) was based on their characteristic GC retention
173 indices and mass spectra. Quantification of lipids was achieved by comparison of
174 mass spectral responses of selected ions (SIM mode, IP₂₅, *m/z* 350; HBI III, *m/z* 346;
175 brassicasterol, *m/z* 470) with those of the internal standards (9-OHD, *m/z* 350; 5α-

176 androstan-3 β -ol, *m/z* 333) and normalized according to their respective response
177 factors and sediment masses (Belt et al. 2012). Analytical reproducibility was
178 monitored using a standard sediment with known abundances of biomarkers for
179 every 20 sediment samples extracted (analytical error 6 %, *n* = 2). PIP₂₅ values were
180 calculated using Equation 1 according to the method of Müller et al. (2011). Similarly,
181 the *c* factor used in the PIP₂₅ calculation was obtained from the ratio of the mean
182 concentrations of IP₂₅ and each phytoplankton biomarker (i.e. brassicasterol and HBI
183 III; Equation 2). Estimates of SpSIC (%) were calculated using the P_{III}IP₂₅ data and
184 the recent calibration of Smik et al. (2016) (Equation 3). Although the study site is
185 located somewhat beyond the main boundary of the region investigated by Smik et
186 al. (2016), we believe that our estimates of SpSIC (and the temporal changes to
187 these) based on this calibration are, nonetheless, realistic, including reasonably
188 good agreement between values from the core-top and known SpSIC obtained from
189 satellite records (see Discussion for further details). A summary of all data can be
190 found in Table 1.

191

$$192 \quad \text{PIP}_{25} = \text{IP}_{25} / (\text{IP}_{25} + cP) \quad (1)$$

$$193 \quad c = \text{mean IP}_{25} / \text{mean P} \quad (2)$$

$$194 \quad \text{SpSIC (\%)} = (\text{P}_{\text{III}}\text{IP}_{25} - 0.0692) / 0.0107 \quad (3)$$

195

196 **3. Results**

197

198 IP₂₅, HBI III and brassicasterol were present in all sedimentary horizons throughout
199 the record although some variability in concentrations was observed for all three
200 biomarkers. Thus, concentrations of IP₂₅, HBI III and brassicasterol were in the

201 ranges 1.6–3.4, 2.2–4.7 and 340–590 ng g⁻¹, respectively (Fig. 2a-c) and all three
202 biomarkers showed a general in-phase fluctuation from ca. 50 to 1750 AD. An
203 increase in IP₂₅, HBI III and brassicasterol concentrations was observed from ca. 5 to
204 400 AD, followed by a decline in all three biomarkers from ca. 400 to 700 AD and an
205 interval of relatively low biomarker concentrations between ca. 700 and 800 AD (Fig.
206 2a-2c). After ca. 800 AD, all biomarkers increased in concentration until ca. 1350
207 AD, before declining again up to ca. 1750 AD. However, a small lag in the decline of
208 IP₂₅ values was observed when compared to those of HBI III and brassicasterol (Fig.
209 2a-2c). In contrast, IP₂₅ concentrations remained generally low after ca. 1750 AD,
210 whereas HBI III and brassicasterol concentrations increased towards the present. In
211 addition, P_{III}IP₂₅ values and estimates of SpSIC (%) values remained reasonably
212 consistent (ca. 0.45–0.57 and 35–45 %, respectively) (Fig. 2d, 2e) between ca. 50
213 and 1400 AD. After ca. 1400 AD, P_{III}IP₂₅ and SpSIC values increased to ca. 0.6 and
214 50 %, respectively, especially between ca. 1500 and 1600 AD, before steadily
215 decreasing towards modern times (Fig. 2d, 2e), where they both reached their lowest
216 values in the entire record.

217

218 **4. Discussion**

219

220 *4.1 Principal outcomes in terms of sea ice conditions*

221

222 The occurrence of the sea ice biomarker IP₂₅ in all sedimentary horizons analysed
223 provides strong evidence that the MSM5/5-712-1 core site experienced seasonal sea
224 ice cover as a consistent hydrographic feature over the last ca. 2 kyr. P_BIP₂₅ and
225 P_{III}IP₂₅ profiles were generally in-phase, indicating that both brassicasterol and HBI

226 III are probably suitable as phytoplankton marker counterparts to IP_{25} for eastern
227 Fram Strait in recent millennia. However, although IP_{25} concentrations and PIP_{25}
228 indices suggest somewhat variable sea ice conditions, the range in our estimates of
229 SpSIC (ca. 25–50%) (Fig. 3d) implies that such variability in sea ice for the West
230 Svalbard margin in recent millennia may have been less extreme than predicted from
231 other proxy records (e.g. Werner et al. 2011), and certainly less than the broad range
232 of sea ice extent for the site throughout the Holocene deduced from a previous study
233 (Müller et al. 2012). For the majority of the early-mid part of the record (ca. 50–1400
234 AD), estimates of SpSIC are reasonably constant (ca. 35–45 %), before an increase
235 to ca. 50% during the period ca. 1500–1600 AD, contemporaneous with the Little Ice
236 Age (Fig. 3d). Following this increase, SpSIC shows a steady reverse trend after ca.
237 1660 AD, which extends to the modern era. Interestingly, this declining trend reflects
238 the general reduction in sea ice and a northward retreat of the maximum winter sea
239 ice extent described in documentary records over the last ca. 150 yr (Divine and Dick
240 2006), while our SpSIC estimates for the top of the core (ca. 25%) are only slightly
241 higher than the mean SpSIC derived from satellite records for this region of Fram
242 Strait over the last ca. 30 yr (10–15 %; NSIDC). Since this interval also corresponds
243 to the upper few centimetres of the core, this slight overestimate in SpSIC might be a
244 consequence of bioturbation in the upper sections, with partial incorporation of older
245 material with higher IP_{25} . Given that $P_{III}IP_{25}$ indices are all well below the lower limit
246 threshold (0.8) suggested recently to be indicative of summer sea ice occurrence
247 (Smik et al., 2016), we also conclude that summer surface waters remained ice-free
248 during the entire record. Further, our data suggest that, since ca. 1900 AD, SpSIC
249 along the West Svalbard margin has diminished to its lowest values in the last 2 kyr,
250 consistent with a coeval and markedly enhanced inflow of warm Atlantic Water to the

251 Arctic Ocean (Spielhagen et al. 2011) and rising air temperatures derived from
252 marine (Rueda et al. 2013) and terrestrial (e.g. D’Andrea et al. 2012) records.

253

254 *4.2 Comparisons with other proxy data*

255

256 The availability of an array of other proxy data for the MSM5/5-712-1 core and
257 related locations enables us to place our new sea ice reconstruction into further
258 context and provide an updated picture of the oceanographic conditions for the West
259 Svalbard margin over the last 2 kyr. Although some consistency between different
260 proxy datasets and alignment with well-known climate epochs (e.g., the Little Ice
261 Age) exists, this is not always the case (e.g. Andersson et al. 2003; Isaksson et al.
262 2005; Werner et al. 2011). As such, we categorise the temporal paleoceanographic
263 evolution for the last 2 kyr into two main intervals, with reference to certain named
264 epochs, where useful.

265

266 *4.2.1 Early-mid part of the record (ca. 50–1750 AD)*

267

268 In the earliest part of the record (ca. 50–700 AD), the increase in IP₂₅, brassicasterol
269 and HBI III concentrations towards ca. 400 AD (Fig. 3a, 3b) suggests a transition
270 from unfavourable conditions for all three biomarkers to one that has a positive
271 influence over the production of both sea ice algae and phytoplankton (viz. ice edge
272 or MIZ conditions). On the basis of enhanced (but variable) planktic foraminiferal
273 fluxes (Fig. 3h), Werner et al. (2011) suggested that this transitional phase
274 represented a general amelioration of conditions from heavy sea ice cover (ca. 120
275 BC to 1 AD) to one with a fluctuating summer ice margin, and our individual

276 biomarker data appear consistent with this interpretation. Further, surface and sub-
277 surface temperatures (Rueda et al. 2013; Spielhagen et al. 2011) increase during
278 this phase (Fig. 3f), which are also indicative of a general reduction in sea ice. In
279 contrast, a decline in all three biomarkers from ca. 400 to 700 AD, is accompanied
280 by a slight cooling trend in the alkenone-derived SST record (Fig. 3f), possibly
281 reflecting a return to increased overall sea ice cover. Indeed, between ca. 700 and
282 800 AD, generally reduced biomarker content coincides with relatively low
283 foraminifera fluxes (Fig. 3h), yet high proportions of polar species (i.e. *N.*
284 *pachyderma*; Werner et al. 2011). Previously, the latter was interpreted as indicating
285 extended sea ice cover, despite there also being evidence for sub-surface advection
286 of Atlantic Water during the same interval (Werner et al. 2011).

287

288 After ca. 800 AD, the increase in all three biomarkers until ca. 1350 AD (Fig. 3a, 3b)
289 suggests a further return to less severe, marginal ice zone (MIZ) conditions, an
290 interpretation supported by a generally warmer surface layer (Fig. 3f) and increases
291 to sub-polar planktic foraminifera (Fig. 3h) (Werner et al. 2011). However, Werner et
292 al. (2011) interpreted the distributions and isotopic composition of planktic
293 foraminifera, together with relatively low IRD from ca. 900 to 1350 AD, as indicative
294 of ice-free conditions, yet our biomarker data suggest seasonal ice cover, even if
295 some estimates of SpSIC from ca. 1100 to 1400 AD are slightly lower (ca. 35 %)
296 than the immediately preceding and subsequent intervals (Fig. 3d). In fact, despite
297 the aforementioned reversible transitions between (apparently) extended sea ice
298 cover and MIZ conditions between ca. 50 and 1300 AD, our estimates of SpSIC
299 remain remarkably consistent (ca. 40%; Fig. 3d) throughout this interval, indicating
300 that factors other than SpSIC are likely to have had influences over biomarker

301 distributions. Although such factors are currently unidentified, it is interesting, for
302 example, that the alternating trend in biomarker concentrations seen between ca. 50
303 and 1350 AD is broadly reflected by the alkenone-derived SST record (Fig. 3f), while
304 the seasonal sea ice dynamics may also exert significant control (see later).

305

306 The decline in all three biomarkers after ca. 1350 AD indicates a possible further
307 return to enhanced sea ice cover and likely marks the transition into the LIA seen in
308 numerous other North Atlantic marine records (e.g. Andersson et al. 2003; Berstad
309 et al. 2003; Eiríksson et al. 2006; Sicre et al. 2011). However, the decline in IP₂₅
310 exhibits a slight lag compared to the phytoplankton markers (Fig. 3a, 3b) suggesting
311 that the transition in sea ice conditions may have been somewhat different to those
312 described previously. This lag in decreasing IP₂₅ concentration is also apparent in
313 the PIP₂₅ data, with maximum values around 1600 AD, reflecting a positive deviation
314 in SpSIC to ca. 50%, before declining to more typical values (ca. 40%) after a further
315 ca. 100 yr (Fig. 3d). In addition, this relatively brief interval of enhanced SpSIC is
316 accompanied by lower SST (alkenone) and sSST (planktic foraminifera) (Fig. 3f).
317 After ca. 1600 AD, a decline in the concentration of all three biomarkers possibly
318 suggests a return to enhanced sea ice cover, despite a reduction in the SpSIC and a
319 slight increase in both SST and sSST (Fig. 3f).

320

321 A clear feature of the temporal fluctuations in individual biomarker concentrations
322 from ca. 0 to 1750 AD is their in-phase temporal coherence (Fig. 3a, 3b),
323 demonstrating that changes to sea ice conditions impacted somewhat equally
324 (directionally) for both IP₂₅ and phytoplankton markers. In some previous IP₂₅-based
325 sea ice reconstructions (e.g. Belt et al. 2015; Cabedo-Sanz et al. 2013; Fahl and

326 Stein 2012; Müller et al. 2009), often opposing trends in IP₂₅ and phytoplankton
327 biomarker profiles have been observed, and interpreted in terms of transitions
328 between intervals of increased sea ice cover (high IP₂₅, low phytoplankton marker)
329 and reduced ice extent (low IP₂₅, high phytoplankton marker). However, consistent
330 with the current data from the West Svalbard margin, Müller et al. (2012) previously
331 reported in-phase changes in IP₂₅ and phytoplankton marker concentrations in a
332 Holocene record from the same site and interpreted such a scenario as indicative of
333 a rapidly fluctuating ice margin. Further, Collins et al. (2013) arrived at a similar
334 conclusion for glacial sea ice conditions in the Southern Ocean, adding that in-phase
335 biomarker trends may also be indicative of low sea ice seasonality. For the current
336 study, such an interpretation may, therefore, represent a preferred alternative to one
337 of a more extreme exchange between extended sea ice cover versus marginal ice
338 zone conditions, as described earlier here, and previously (Werner et al. 2011),
339 especially since IP₂₅ and the phytoplankton markers are all present throughout the
340 record. In addition, our estimates of SpSIC (ca. 35–45 %) (Fig. 3d) and previous
341 determinations of sea ice duration (ca. 2–6 months/yr) (Fig. 3e) based on dinocysts
342 in a core from the same site (Bonnet et al. 2010), both indicate seasonal, rather than
343 extended, ice cover. In-phase trends within individual biomarker profiles generally
344 have the impact of reducing variability in PIP₂₅ (and SpSIC) that may, potentially,
345 lead to an underestimation of the changes in sea ice conditions implied from IP₂₅
346 alone. However, for the MSM5/5-712-1 core, changes in IP₂₅ concentration are also
347 relatively small, especially when compared to those seen in longer Holocene records
348 from the same and nearby sites (MSM5/5-712-2 and MSM5/5-723-2; Müller et al.
349 2012), both of which exhibit similar IP₂₅ profiles to our data for the overlapping period
350 (Fig. 3a). Thus, IP₂₅ concentration changes by an order of magnitude from the early

351 to late Holocene in the MSM5/5-712-2 record (Müller et al. 2012), while values
352 covering the last ca. 2 kyr in all three cores only vary by a factor of two, at most (Fig.
353 3a). Of course, a fluctuating ice margin has much closer parallels with the modern
354 sea ice cycle for the region, with a significantly smaller change in the position of the
355 winter and summer ice margins than, for example, the neighboring Barents Sea (Fig.
356 1a). Interestingly, peak total foraminifera fluxes (Fig. 3h), previously interpreted as
357 representing ice edge settings by comparison with modern datasets (Werner et al.
358 2011), also broadly coincide with increased biomarker concentrations, consistent
359 with a strong biological coupling between the surface and sub-surface environments.

360

361 4.2.2 The last 250 years (since ca. 1750 AD)

362

363 According to our biomarker data, conditions after ca. 1750 AD did not parallel the
364 early-mid part of the record, with generally low IP_{25} concentrations accompanied by
365 increasing phytoplankton marker abundances, especially after ca. 1800 AD. Such
366 changes are particularly apparent through declining PIP_{25} values and SpSIC, but it is
367 also evident that surface (alkenone) and sub-surface (planktic foraminifera)
368 temperatures diverge during this latter part of the LIA, with a clear cooling trend
369 observed for the former (Fig. 3f). The occurrence of generally opposing trends
370 between IP_{25} and HBI III (and brassicasterol) since ca. 1750 AD contrasts the earlier
371 part of the record and previous longer-term Holocene sea ice records from the region
372 (Müller et al. 2012). However, this divergence in IP_{25} and phytoplankton biomarkers
373 is reminiscent of the distributions of IP_{25} and HBI III in surface sediments and
374 downcore records (e.g. core sites 11 and 70; Fig. 1a) from the Barents Sea, with low
375 IP_{25} and high HBI III, in particular, associated with ice-edge retreat within the MIZ

376 during spring (Belt et al., 2015). We suggest, therefore, that from ca. 1750 AD to
377 modern, surface conditions at the West Svalbard margin transcended from higher
378 seasonal sea ice cover (i.e. ca. 40% SpSIC), to a winter ice-edge scenario with
379 reduced SpSIC (ca. 25% or less).

380

381 Our observation of declining SpSIC since ca. 1600 AD is also consistent with the
382 suggestion by Rueda et al. (2013) that reduced surface temperatures and increasing
383 air and sub-surface temperatures, especially in the last ca. 500 yr, may have
384 coincided with a trend of increasing sea ice melt and thus, SpSIC. Increased air
385 temperatures have also been reconstructed for neighboring (terrestrial) West
386 Spitsbergen, with concomitant glacial advance attributed to enhanced precipitation
387 (D’Andrea et al. 2012) that we suggest may also have been associated with reduced
388 sea ice cover. Alternatively, lower SSTs in the recent record may reflect an earlier
389 seasonal bloom due to lower sea ice conditions as suggested previously to explain
390 apparent anomalies in SSTs for the North Icelandic Shelf and coastal settings
391 around Newfoundland in the Labrador Sea (Sicre et al. 2011, 2014). In any case, the
392 apparently increased de-coupling between the surface and sub-surface temperature
393 records since ca. 1750 AD likely reflects a period of most significant change in sea
394 ice conditions, with cooler and fresher surface waters resulting from melting sea ice,
395 possibly as a result of warmer air temperatures as suggested by Rueda et al. (2013).
396 It is also noted that IRD content reached its highest values after ca. 1750 AD (Fig.
397 3g), a further indicator of increasing sea ice melt, although an additional contribution
398 to the IRD budget from icebergs derived from Svalbard glaciers cannot be
399 discounted (e.g. Andersen et al. 1996; Werner et al. 2011).

400

401 4.2.3 Biomarker versus dinocyst approaches to sea ice reconstruction

402

403 As a final discussion point, we compare our biomarker-based sea ice reconstruction
404 with one based on dinocysts in a further core obtained from the same site (Fig. 3e;
405 Bonnet et al. 2010). Inspection of the temporal profile for dinocyst-based sea ice
406 duration (Fig. 3e) with those of biomarkers (individual or PIP₂₅; Fig. 3a-3c) or SpSIC
407 (Fig. 3d) reveals no clear or consistent agreement, even factoring in potential age-
408 control offsets between the two cores. Although some parallels might exist in the
409 early-mid parts of the dinocyst and SpSIC records (ca. 50 to 1400 AD; Fig.3d, 3e),
410 this is not the case for the later profiles, and after ca. 1600 AD, in particular, with
411 reconstructions exhibiting generally opposing trends. In the most recent parts of the
412 records, for example, our estimates of lowest SpSIC align with the northerly retreat
413 of the winter sea ice margin over the last ca. 150 yr (Fig. 1b; Divine and Dick 2006),
414 yet apparently contradict an enhancement in sea ice duration in the dinocyst record
415 (Fig. 3e). Further, the reconstruction of Bonnet et al. (2010) implies ice-free
416 conditions ca. 550–700 AD, while our data suggest SpSIC of ca. 40% for the same
417 interval. Inconsistencies in proxy records are not uncommon, however, and a
418 number of discrepancies have already been reported and discussed for surface
419 temperature and salinity reconstructions based on foraminifera and dinocysts in
420 different cores from the study location (Bonnet et al. 2010; Werner et al. 2011). Such
421 differences are not necessarily straightforward to resolve, but may potentially arise
422 from influences associated with seasonally-dependent proxy responses, changes to
423 water column sub-structure, variable depth habitat of native flora and fauna, or
424 appropriateness of transfer functions, which may exhibit a strong regional
425 dependence. Inconsistencies between biomarker- and dinocyst-based sea ice

426 reconstructions have been reported previously and loosely attributed to the possible
427 different signatures that each proxy represents (e.g. Belt and Müller 2013; de Vernal
428 et al. 2013a; Ledu et al. 2010; Polyak et al. in press). Outcomes from the current
429 study might help further direct this debate. For example, the dinocyst-based method
430 yields semi-quantitative estimates of sea ice *duration* in months of sea ice (with >50
431 % cover)/yr (de Vernal et al. 2013b), while the corresponding reconstructions based
432 on IP₂₅ are intrinsically associated with spring sea ice conditions (Belt et al. 2013;
433 Brown et al. 2011) and, more quantitatively, seasonal (spring) sea ice *concentration*,
434 as described here and previously (Belt et al. 2015; Müller et al. 2011; Navarro-
435 Rodriguez et al. 2013; Smik et al. 2016; Xiao et al. 2015). For the current study, we
436 also note that SpSIC is almost exclusively below the threshold level for dinocyst-
437 based methods (>50% sea ice cover) in any case, so differences between outcomes
438 are not entirely unexpected. It is also feasible that while there might be some
439 scenarios for which sea ice duration and SpSIC are reasonably in-phase, divergence
440 in their respective proxy records may reflect an effective de-coupling between them,
441 especially during intervals of amplified seasonality. For example, for the West
442 Svalbard margin, we speculate that increasing sea ice duration, yet declining SpSIC,
443 seen in the last ca. 300 years, may have arisen due to larger seasonal shifts
444 between generally colder winters and warmer summer temperatures that would have
445 particularly impacted on spring ice melt. Consistent with this suggestion, increasing
446 air temperatures from marine (Rueda et al. 2013) and terrestrial (D’Andrea et al.
447 2012) records for the region since ca. 1600 AD coincide with the reduction in SpSIC
448 shown here. The combination of new biomarker-based approaches for estimating
449 SpSIC with complementary methods of determining sea ice duration may, therefore,
450 offer additional insights into seasonal shifts in sea ice occurrence that are not

451 necessarily available from either individual proxy. Such approaches would clearly
452 benefit from further dinocyst and biomarker investigations on the same sediments.

453

454 **5. Conclusions**

455

456 Our biomarker-based reconstruction of sea ice conditions for the West Svalbard
457 continental margin covering the last ca. 2 kyr, suggests that changes to sea ice
458 conditions during this interval may not have been as extreme as reported in previous
459 proxy-based studies, especially for the interval ca. 50–1700 AD, with SpSIC
460 generally ca. 40% throughout. An increase in SpSIC to ca. 50% was observed at ca.
461 1600 AD, however, which we attribute to slightly enhanced sea ice cover during the
462 LIA. SpSIC returned to more typical values at ca. 1750 AD, before declining further
463 towards modern values (ca. 25%), consistent with observational records of a
464 northerly retreat of the winter sea ice limit in the last ca. 150 yr (Divine and Dick
465 2006). The general in-phase behavior of the sea ice algal and phytoplankton
466 markers observed for the majority of the record (ca. 50–1750 AD), is indicative of a
467 fluctuating ice margin and relatively low sea ice seasonality. In contrast, a
468 divergence in trends of the same biomarkers since ca. 1750 AD is interpreted in
469 terms of an amplified seasonal sea ice cycle and a rapid ice edge retreat within the
470 MIZ during the spring; thus providing a model for the sea ice conditions for the West
471 Svalbard margin in recent centuries. Such a contrast in the relative temporal trends
472 of sea ice and pelagic biomarkers has been observed in related sea ice
473 reconstructions (e.g. Belt et al. 2015; Müller et al. 2009) and may prove to be an
474 additionally useful tool when deducing or refining paleo sea ice conditions.
475 Improvements to such paleo sea ice descriptions, and temporal changes to these,

476 will also help in the further refinement of other proxy-based inferences of surface
477 environments, in particular, and may potentially help clarify (or resolve)
478 reconstructions of broader water column features for sea ice covered settings.

479

480 **6. Acknowledgements**

481

482 We thank the University of Plymouth for financial support and Dr Robert Spielhagen
483 for sampling the MSM5/5-712-1 core. We are also grateful to two anonymous
484 reviewers who provided a number of useful comments that helped improve the
485 quality of the manuscript. This work is a contribution to the CASE Initial Training
486 Network funded by the European Community's 7th Framework Programme FP7
487 2007/2013, Marie-Curie Actions, under Grant Agreement No. 238111.

488 7. References

- 489 Andersen ES, Dokken TM, Elverhøi A, Solheim A, Fossen I (1996) Late Quaternary
490 sedimentation and glacial history of the western Svalbard continental margin *Marine*
491 *Geology* 133:123-156
- 492 Andersson C, Risebrobakken B, Jansen E, Dahl SO (2003) Late Holocene surface
493 ocean conditions of the Norwegian Sea (Vøring Plateau) *Paleoceanography* 18:1044
- 494 Belt ST, Allard WG, Massé G, Robert J-M, Rowland SJ (2000) Highly branched
495 isoprenoids (HBIs): identification of the most common and abundant sedimentary
496 isomers *Geochimica et Cosmochimica Acta* 64:3839-3851
- 497 Belt ST, Brown TA, Navarro Rodriguez A, Cabedo Sanz P, Tonkin A, Ingle R (2012)
498 A reproducible method for the extraction, identification and quantification of the Arctic
499 sea ice proxy IP₂₅ from marine sediments *Analytical Methods* 4:705-713
- 500 Belt ST, Brown TA, Ringrose AE, Cabedo-Sanz P, Mundy CJ, Gosselin M, Poulin M
501 (2013) Quantitative measurement of the sea ice diatom biomarker IP₂₅ and sterols in
502 Arctic sea ice and underlying sediments: Further considerations for palaeo sea ice
503 reconstruction *Organic Geochemistry* 62:33-45
- 504 Belt ST, Cabedo-Sanz P, Smik L, Navarro-Rodriguez A, Berben SM, Knies J, Husum
505 K (2015) Identification of paleo Arctic winter sea ice limits and the marginal ice zone:
506 Optimised biomarker-based reconstructions of late Quaternary Arctic sea ice *Earth*
507 *and Planetary Science Letters* 431:127-139
- 508 Belt ST, Massé G, Rowland SJ, Poulin M, Michel C, LeBlanc B (2007) A novel
509 chemical fossil of palaeo sea ice: IP₂₅ *Organic Geochemistry* 38:16-27
- 510 Belt ST, Müller J (2013) The Arctic sea ice biomarker IP₂₅: a review of current
511 understanding, recommendations for future research and applications in palaeo sea
512 ice reconstructions *Quaternary Science Reviews* 79:9-25
- 513 Belt ST et al. (2010) Striking similarities in temporal changes to spring sea ice
514 occurrence across the central Canadian Arctic Archipelago over the last 7000 years
515 *Quaternary Science Reviews* 29:3489-3504
- 516 Berben SMP, Husum K, Cabedo-Sanz P, Belt ST (2014) Holocene sub centennial
517 evolution of Atlantic water inflow and sea ice distribution in the western Barents Sea
518 *Climate of the Past* 10:181-198
- 519 Berstad IM, Sejrup HP, Klitgaard - Kristensen D, Hafliðason H (2003) Variability in
520 temperature and geometry of the Norwegian Current over the past 600 yr; stable
521 isotope and grain size evidence from the Norwegian margin *Journal of Quaternary*
522 *Science* 18:591-602

- 523 Bonnet S, de Vernal A, Hillaire-Marcel C, Radi T, Husum K (2010) Variability of sea-
524 surface temperature and sea-ice cover in the Fram Strait over the last two millennia
525 *Marine Micropaleontology* 74:59-74
- 526 Brown TA, Belt ST (2012) Identification of the sea ice diatom biomarker IP₂₅ in Arctic
527 benthic macrofauna: direct evidence for a sea ice diatom diet in Arctic heterotrophs
528 *Polar Biology* 35:131-137
- 529 Brown TA, Belt ST, Philippe B, Mundy CJ, Massé G, Poulin M, Gosselin M (2011)
530 Temporal and vertical variations of lipid biomarkers during a bottom ice diatom
531 bloom in the Canadian Beaufort Sea: further evidence for the use of the IP₂₅
532 biomarker as a proxy for spring Arctic sea ice *Polar Biology* 34:1857-1868
- 533 Brown TA, Belt ST, Tatarek A, Mundy CJ (2014) Source identification of the Arctic
534 sea ice proxy IP₂₅ *Nature communications* 5
- 535 Cabedo-Sanz P, Belt ST, Knies J, Husum K (2013) Identification of contrasting
536 seasonal sea ice conditions during the Younger Dryas *Quaternary Science Reviews*
537 79:74-86
- 538 Collins LG, Allen CS, Pike J, Hodgson DA, Weckström K, Massé G (2013)
539 Evaluating highly branched isoprenoid (HBI) biomarkers as a novel Antarctic sea-ice
540 proxy in deep ocean glacial age sediments *Quaternary Science Reviews* 79:87-98
- 541 D'Andrea WJ, Vaillencourt DA, Balascio NL, Werner A, Roof SR, Retelle M, Bradley
542 RS (2012) Mild Little Ice Age and unprecedented recent warmth in an 1800 year lake
543 sediment record from Svalbard *Geology* 40:1007-1010
- 544 de Vernal A, Gersonde R, Goosse H, Seidenkrantz M-S, Wolff EW (2013a) Sea ice
545 in the paleoclimate system: the challenge of reconstructing sea ice from proxies – an
546 introduction *Quaternary Science Reviews* 79:1-8
- 547 de Vernal A, Rochon A, Fréchette B, Henry M, Radi T, Solignac S (2013b)
548 Reconstructing past sea ice cover of the Northern Hemisphere from dinocyst
549 assemblages: status of the approach *Quaternary Science Reviews* 79:122-134
- 550 Dickson R, Rudels B, Dye S, Karcher M, Meincke J, Yashayaev I (2007) Current
551 estimates of freshwater flux through Arctic and subarctic seas *Progress in*
552 *Oceanography* 73:210-230
- 553 Divine DV, Dick C (2006) Historical variability of sea ice edge position in the Nordic
554 Seas *J Geophys Res* 111:C01001
- 555 Eiriksson J et al. (2006) Variability of the North Atlantic Current during the last 2000
556 years based on shelf bottom water and sea surface temperatures along an open
557 ocean/shallow marine transect in western Europe *The Holocene* 16:1017-1029

- 558 Fahl K, Stein R (2012) Modern seasonal variability and deglacial/Holocene change
559 of central Arctic Ocean sea-ice cover: New insights from biomarker proxy records
560 Earth and Planetary Science Letters 351–352:123-133
- 561 Goosse H, Roche DM, Mairesse A, Berger M (2013) Modelling past sea ice changes
562 Quaternary Science Reviews 79:191-206
- 563 Hopkins TS (1991) The GIN Sea - a synthesis of its physical oceanography and
564 literature review 1972 - 1985 Earth Science Reviews 30:175-318
- 565 Isaksson E et al. (2005) Two ice-core $\delta^{18}\text{O}$ records from Svalbard illustrating climate
566 and sea-ice variability over the last 400 years The Holocene 15:501-509
- 567 Jernas P, Klitgaard Kristensen D, Husum K, Wilson L, Koç N (2013)
568 Palaeoenvironmental changes of the last two millennia on the western and northern
569 Svalbard shelf Boreas 42:236-255
- 570 Johannessen OM et al. (2004) Arctic climate change: observed and modelled
571 temperature and sea ice variability Tellus A 56:328-341
- 572 Ledu D, Rochon A, de Vernal A, St-Onge G (2010) Holocene paleoceanography of
573 the northwest passage, Canadian Arctic Archipelago Quaternary Science Reviews
574 29:3468-3488
- 575 Loeng H (1991) Features of the physical oceanographic conditions of the Barents
576 Sea Polar research 10:5-18
- 577 Müller J, Massé G, Stein R, Belt ST (2009) Variability of sea-ice conditions in the
578 Fram Strait over the past 30,000 years Nature Geoscience 2:772-776
- 579 Müller J, Stein R (2014) High-resolution record of late glacial and deglacial sea ice
580 changes in Fram Strait corroborates ice–ocean interactions during abrupt climate
581 shifts Earth and Planetary Science Letters 403:446-455
- 582 Müller J, Wagner A, Fahl K, Stein R, Prange M, Lohmann G (2011) Towards
583 quantitative sea ice reconstructions in the northern North Atlantic: A combined
584 biomarker and numerical modelling approach Earth and Planetary Science Letters
585 306:137-148
- 586 Müller J, Werner K, Stein R, Fahl K, Moros M, Jansen E (2012) Holocene cooling
587 culminates in sea ice oscillations in Fram Strait Quaternary Science Reviews 47:1-14
- 588 Navarro-Rodriguez A, Belt ST, Knies J, Brown TA (2013) Mapping recent sea ice
589 conditions in the Barents Sea using the proxy biomarker IP_{25} : implications for palaeo
590 sea ice reconstructions Quaternary Science Reviews 79:26-39

- 591 Polyak L, Belt ST, Cabedo-Sanz P, Yamamoto M, Park Y-H (in press) Holocene sea-
592 ice conditions and circulation at the Chuckchi-Alaskan margin, Arctic Ocean, inferred
593 from biomarker proxies *The Holocene*
- 594 Rueda G, Fietz S, Rosell-Melé A (2013) Coupling of air and sea surface
595 temperatures in the eastern Fram Strait during the last 2000 years *The Holocene*
596 23(5):692-698
- 597 Sicre MA et al. (2011) Sea surface temperature variability in the subpolar Atlantic
598 over the last two millennia *Paleoceanography* 26:PA4218
- 599 Sicre MA et al. (2014) Labrador current variability over the last 2000 years *Earth and*
600 *Planetary Science Letters* 400:26-32
- 601 Smik L, Cabedo-Sanz P, Belt ST (2016) Semi-quantitative estimates of paleo Arctic
602 sea ice concentration based on source-specific highly branched isoprenoid alkenes:
603 A further development of the PIP₂₅ index *Organic Geochemistry* 92:63-69
- 604 Spielhagen RF et al. (2011) Enhanced modern heat transfer to the Arctic by warm
605 Atlantic water *Science* 331:450-453
- 606 Stein R, Fahl K, Müller J (2012) Proxy Reconstruction of Cenozoic Arctic Ocean
607 Sea-Ice History—from IRD to IP₂₅— *Polarforschung* 82:37-71
- 608 Stoyanova V, Shanahan TM, Hughen KA, de Vernal A (2013) Insights into Circum-
609 Arctic sea ice variability from molecular geochemistry *Quaternary Science Reviews*
610 79:63-73
- 611 Stroeve JC, Serreze MC, Holland MM, Kay JE, Malanik J, Barrett AP (2012) The
612 Arctic's rapidly shrinking sea ice cover: a research synthesis *Climatic Change*
613 110:1005-1027
- 614 Thomas DN, Dieckmann GS (2010) *Sea Ice*. second edn. Wiley Blackwell
615 Publishing, New York
- 616 Vinje T (1975) Sea ice conditions in the European sector of the marginal seas of the
617 Arctic, 1966–1975 *Norsk Polarinst, Arbok*:163-174
- 618 Werner K, Spielhagen RF, Bauch D, Hass HC, Kandiano E (2013) Atlantic Water
619 advection versus sea - ice advances in the eastern Fram Strait during the last 9 ka:
620 Multiproxy evidence for a two - phase Holocene *Paleoceanography* 28:283-295
- 621 Werner K, Spielhagen RF, Bauch D, Hass HC, Kandiano E, Zamelczyk K (2011)
622 Atlantic Water advection to the eastern Fram Strait—Multiproxy evidence for late
623 Holocene variability *Palaeogeography, Palaeoclimatology, Palaeoecology* 308:264-
624 276

- 625 Xiao X, Fahl K, Müller J, Stein R (2015) Sea-ice distribution in the modern Arctic
626 Ocean: Biomarker records from trans-Arctic Ocean surface sediments *Geochimica et*
627 *Cosmochimica Acta* 155:16-29
- 628 Xiao X, Fahl K, Stein R (2013) Biomarker distributions in surface sediments from the
629 Kara and Laptev seas (Arctic Ocean): indicators for organic-carbon sources and sea-
630 ice coverage *Quaternary Science Reviews* 79:40-52

8. Figure Legends

Figure 1: (a) Map showing the core location under study (yellow diamond): MSM5/5-712-1 (712-1). Other cores mentioned in this paper (black dots) are: MSM5/5-723-2 (723-2, Müller et al. 2012), MSM5/5-712-2 (712-2, Müller et al. 2012), JM09-KA11-GC (11, Belt et al. 2015) and NP05-11-70GC (70, Belt et al. 2015). The core site described in Bonnet et al. (2010) is at the same location as core 712-1. The main ocean currents are the cold East Greenland Current (EGC), carried southwards along the east coast of Greenland, and the relatively warm North Atlantic Current (NAC) that flows northward along the northern Norwegian shelf and continues into the Arctic Ocean via the West Spitsbergen Current (WSC). The cold East Spitsbergen Current (ESC) is also indicated. The median sea ice extent (>15% monthly mean concentration) for March (black line) and September (magenta line) are shown for the period 1981–2010 (National Snow and Ice Data Center, Boulder, Colorado); (b) Map showing average April location of the sea ice margins at 1870–1920 AD (black line), 1921–1961 AD (blue line), 1962–1988 AD (magenta line) and 1989–2002 AD (red line), (<http://nsidc.org/data/gis/data.html>; data based on Divine and Dick, 2006). The five ¹⁴C accelerator mass spectrometry (AMS) radiocarbon dates used for the age model (Spielhagen et al. 2011) are shown as black diamonds.

Figure 2: Temporal concentration profiles of (a) IP₂₅; (b) HBI III; (c) Brassicasterol; (d) PIP₂₅ indices calculated using phytoplankton markers HBI III (P_{III}IP₂₅) and brassicasterol (P_BIP₂₅); (e) SpSIC (%) based on Smik et al. (2016).

Figure 3. Compilation of proxy data from MSM5/5-712-1 and related cores from the study region. Data are for MSM5/5-712-1 unless otherwise stated. (a) IP_{25} concentrations in MSM5/5-712-1 (black line), MSM5/5-712-2 (red line, Müller et al. 2012) and MSM5/5-723-2 (blue line, Müller et al. 2012); (b) HBI III and brassicasterol concentrations; (c) PIP_{25} indices calculated using phytoplankton markers HBI III ($P_{III}IP_{25}$) and brassicasterol ($P_{BI}IP_{25}$); (d) SpSIC (%) based on Smik et al. (2016); (e) Dinocyst-based sea ice cover (months/yr) derived from a further core at the same location as MSM5/5-712-1 (Bonnet et al. 2010); (f) SST and sSST ($^{\circ}C$) derived from alkenones (Rueda et al. 2013) and planktic foraminifera (Spielhagen et al. 2011), respectively; (g) IRD in the 150–250 μm fraction (Werner et al. 2011); (h) fluxes of polar and subpolar planktic foraminifers (100–250 μm fraction) (Spielhagen et al. 2011; Werner et al. 2011). The five ^{14}C accelerator mass spectrometry (AMS) radiocarbon dates used for the age model (Spielhagen et al. 2011) are shown as black diamonds.

Figure 1:

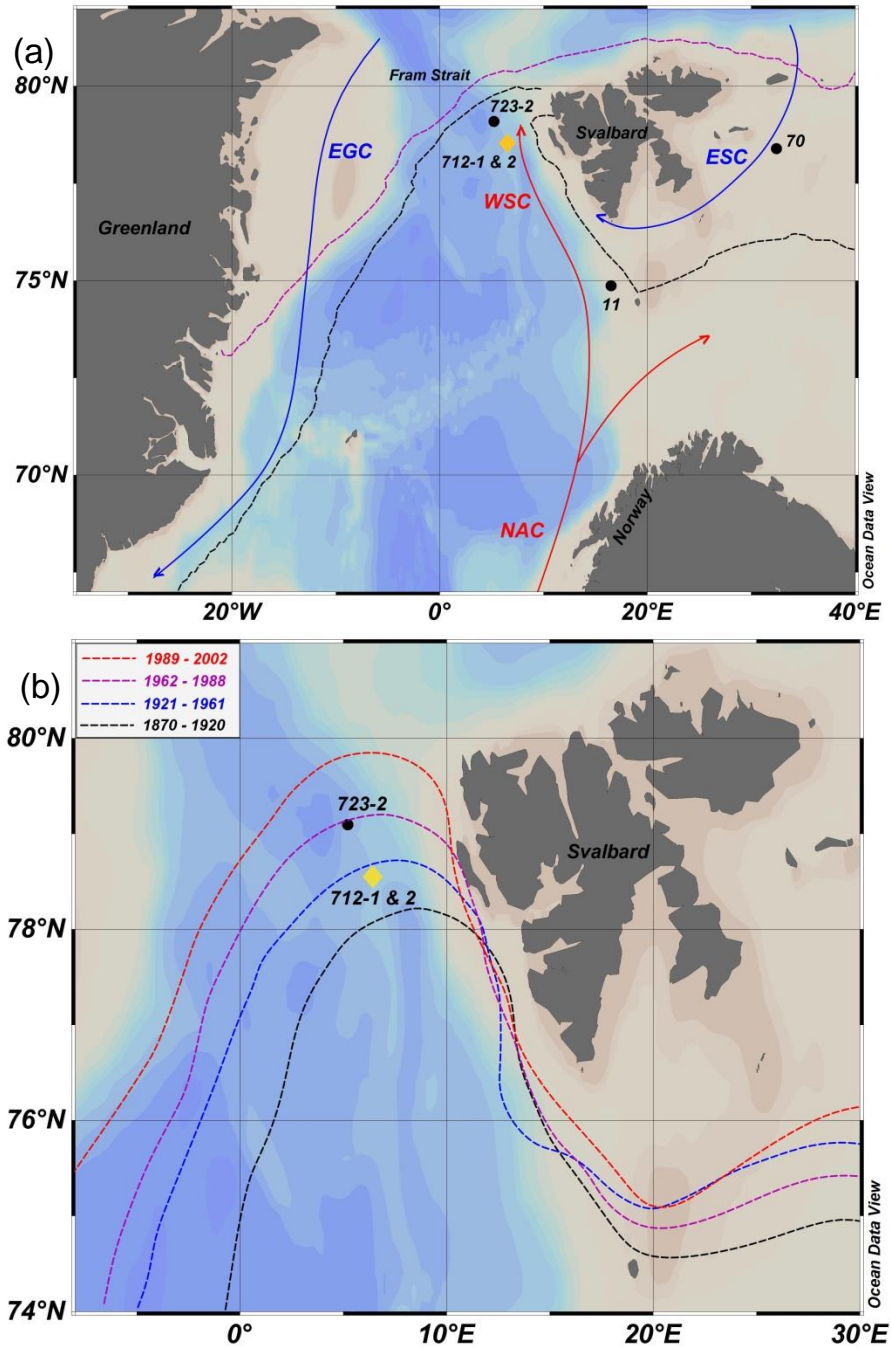


Figure 2:

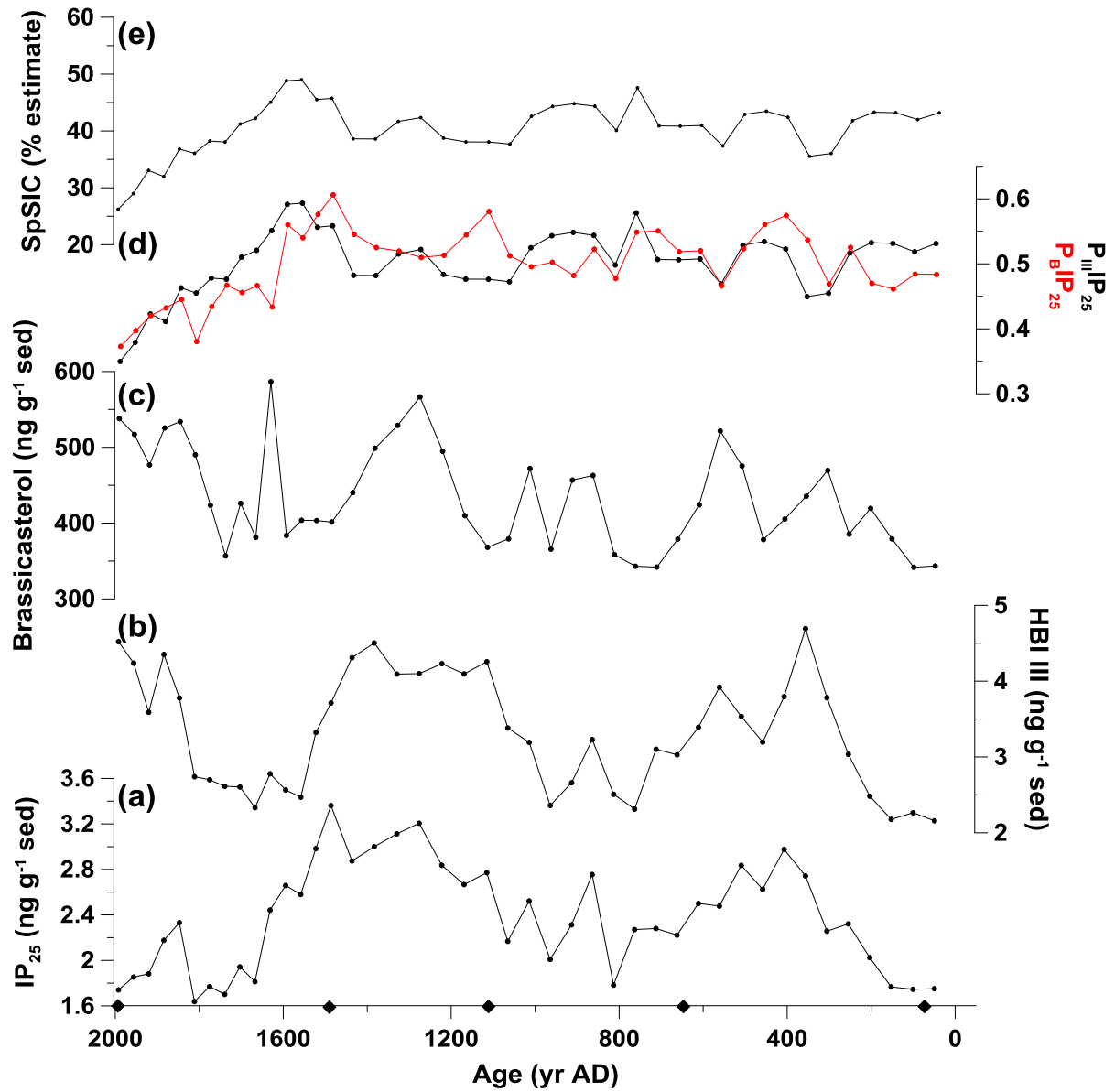


Figure 3:

